INSTABILITY AND COLLAPSE OF FLEXIBLY-CONNECTED GABLED FRAMES

G. J. SIMITSES† and S. E. MOHAMED

School of Aerospace Engineering, Georgia Institute of Technology, Atlanta, GA 30332, U.S.A.

Abstract—A nonlinear elasto-plastic instability analysis of flexibly connected and supported gabled frames with uniform and nonuniform geometry is presented. The analysis incorporates stability and strength. The procedure is based on nonlinear kinematic relations and linearly elastic material behavior except at the plastic regions (concentrated plasticity). The nonlinear flexible connections are represented by polynomial models. Thus, various types of response can be predicted. Through the chosen examples, the following types of response have been observed: elastic bifurcation instability, elastic limit point instability, elasto-plastic limit point instability and plastic collapse. The effect of several parameters is assessed in order to enhance our understanding of frame behavior. These include the effects of nonuniform geometry, of rotational restraints at the supports, of rise to span ratio, of beam to column stiffness ratio, of load eccentricity and of joint flexible connections.

NOMENCLATURE

A_i	cross-sectional area of bar i
A_{ij}	coefficient of general solution to equilibrium differential equation of bar i
A_{ij}^*	coefficient of general solution to buckling differential equation of bar i
e_i	load eccentricity in bar i
e_{xx}	extensional strain
E	modulus of elasticity
F_Y	yield stress
I_i	second moment of area of bar i
k_i^2	$P_i L_i^2/EI_i$
$\bar{k}_i$	k_i on primary equilibrium path
k_i^*	$P_i^* L_i^2/EI_i$
L	column height
L_i	length of bar i
M_i	bending moment in bar i
M_{PC}	plastic moment capacity
M_P	full plastic moment capacity
P_Y	yield stress times member area
P_i	axial force in bar i
P_i^*	additional P_i corresponding to U_i^*, W_i^*
q_i	uniformly distributed load on bar i
Q_i	concentrated load on bar i
S	span of the gabled frame
t, g, d	size parameters for the particular connection considered
U_T	total potential energy
u_i	axial displacement component along bar i
U_i	u_i/L_i
U_i^*	kinematically admissible variation of U_i
V_i	shearing force of bar i
w_i	in-plane normal displacement component along bar i
W_i	w_i/L_i
W_i^*	kinematically admissible variation of W_i
x_i	axial coordinate of bar i
Z_P	plastic modulus
β	rotational spring stiffness at the support
η	potential energy of external forces
λ_i	slenderness ratio of bar i
ϕ	relative rotation in the connection

1. INTRODUCTION

Considerable research has been devoted to understanding the true behavior of framed structures. This research has involved finding the elastic critical load (bifurcation or limit point) (see Oran, 1973; Qashu and Dadeppo, 1983; Simitses and Giri, 1981; Simitses and Kounadis, 1978; Simitses and Mohamed, 1988; Simitses and Vlahinos, 1982) or plastic collapse load (see Jennings and Majid, 1965; Kassimali, 1968; Korn and Galambos, 1968;

† Presently Head of Department of Aerospace Engineering and Engineering Mechanics, University of Cincinnati, Cincinnati, OH 45221, U.S.A.
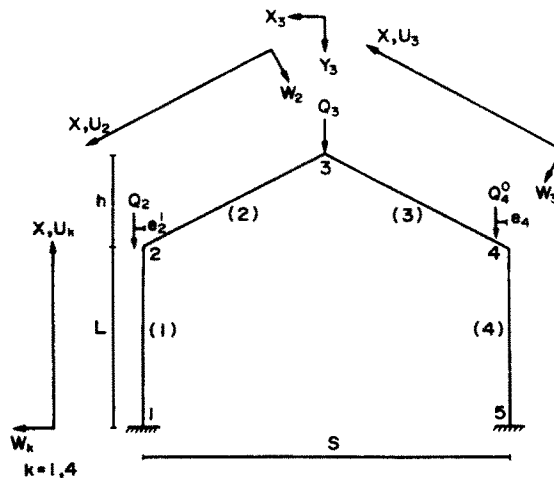
Fig. 1. Geometry and sign convention.

Lui, 1985). The second-order elastic–plastic analysis is considered a very good approach to predict the true behavior of a practical frame. So, some researchers have employed the second-order elastic–plastic analysis by using the slope deflection (Kassimali, 1968; Korn and Galambos, 1968) method, others by using the stiffness method (Lui, 1985). Most of these works deal with orthogonal frames without considering the possibility of sway buckling instability or limit point instability before plastic collapse. Moreover, very few investigators have considered additionally the effect of connection flexibility on the behavior of the frame (Lui, 1985).

The objective of this paper is to present a nonlinear elastic–plastic analysis of gabled frames with uniform and nonuniform geometry, and with or without semirigid connections or elastic–rotational restraints at the supports. Another objective is to show that both stability and strength must be incorporated into the analysis in order to fully understand the behavior of frames.

2. METHOD OF ANALYSIS

The analysis is based on nonlinear kinematic relations and linearly elastic material behavior except at plastic regions (concentrated plasticity). The material is assumed to behave as elastic–perfectly plastic, and yielding is considered to be concentrated at member ends. The influence of axial force on the plastic moment capacity is considered. All the displacements are assumed to be in the plane of the frame. The cross-section perpendicular to the longitudinal fibers before deformation is assumed to remain perpendicular to the deformed longitudinal fibers. The plastic hinge is assumed to become a real hinge.

3. MATERIAL FORMULATION

Consider the gabled frame shown in Fig. 1. Each bar is of length L_i, cross-section area A_i, and of second moment of area I_i. The sign convention associated with the bar in-plane and normal displacement components, u_i (along the length, x_i) and w_i (normal to the bar) is shown in Fig. 1. The external loads, Q_i, q_i, applied to the frame consist of concentrated loads and uniformly distributed loads normal to the respective bar. The load eccentricity e_i is positive in the positive direction of the coordinate system. Superscript zero identified the eccentricity at $X = 0$ and superscript 1 at $X = 1$ (see Fig. 1).

3.1. Equilibrium equations and related conditions (elastic response)

Through the principle of the stationary value of the total potential, one may derive the following equilibrium equations and associated end conditions:

$$EA_i[u_{i,x} + \tfrac{1}{2}(w_{i,x})^2]_{,x} = 0 \tag{1}$$

$$EI_i w_{i,xxxx} - EA_i[u_{i,x} + \tfrac{1}{2}(w_{i,x})^2]w_{i,xx} = q_i, \tag{2}$$

for $i = 1, 2, 3, \ldots, N$.

The expressions for the boundary and auxiliary joint (kinematic continuity and joint balance of forces and moments) conditions can be deduced from those found in Simitses and Mohamed (1988) and Simitses and Vlahinos (1982). They are not shown herein for the sake of brevity.

The displacement components u_i and w_i are functions of the coordinate x. One may express the internal forces and moments (P_i, V_i and M_i), acting on a cross-section normal to the undeflected axis of the member as follows:

$$P_i(x) = EA_i[u_{i,x} + \tfrac{1}{2}(w_{i,x})^2]$$
$$M_i(x) = EI_i w_{i,xx}$$
$$V_i(x) = EA_i[u_{i,x} + \tfrac{1}{2}(w_{i,x})^2]w_{i,x} - EI_i w_{i,xxx}. \tag{3}$$

The following nondimensionalized parameters are introduced for convenience:

$$X = x/L_i \quad \bar{q}_i = q_i L_i^3/EI_i \quad k_i^2 = \mp(P_i L_i^2)/EI \quad U_i = u_i/L_i$$

$$q_i^* = q_i L^3/EI_1 \quad \lambda_i = L_i/\sqrt{I_i/A_i} \quad W_i = w_i/L_i \quad \bar{Q}_i = Q_i L^2/EI_1,$$

$$S_i = (EI_i L)/(EI_1 L_i) \quad \bar{e}_i = e_i/L \quad \bar{\beta}_i = \beta_i L/EI_1 \quad R_i = L_i/L$$

$$\bar{M}_{PC} = M_{PC} L/EI_1 \quad \bar{P}_Y = P_Y L^2/EI_1. \tag{4}$$

Thus, the expressions for the forces and moments in terms of these nondimensionalized parameters are:

$$Q_i = \bar{Q}_i EI_1/L^2, \quad P_i = \mp k_i^2 EI_i/(L_i)^2, \quad q_i = q_i^* EI_1/(L)^3$$
$$M_i = W_{i,XX} EI_i/L_i, \quad V_i = [\mp k_i^2 W_{i,X} - W_{i,XXX}]EI_i/L_i^2. \tag{5}$$

The top sign holds for the case for which the ith bar is in compression (P_i is positive in tension and negative in compression). From eqns (1) and (2) one may express the equilibrium equations in nondimensionalized form as follows:

$$U_{i,X} + 1/2(W_{i,X})^2 = \mp k_i^2/\lambda_i^2 \tag{6}$$

$$W_{i,XXXX} \pm k_i^2 W_{i,XX} = \bar{q}_i. \tag{7}$$

The solution to the above equilibrium equations is given by:

(for compression)

$$U_i(X) = A_{i5} - k_i^2 X/\lambda_i^2 - 1/2 \int_0^X [W_{i,X}(X)]^2 \, dX \tag{8}$$

$$W_i(X) = A_{i1} \sin k_i X + A_{i2} \cos k_i X + A_{i3} X + \bar{q}_i X^2/(2k_i^2) + A_{i4}, \tag{9}$$

(for tension)

$$U_i(X) = A_{i5} + k_i^2 X/\lambda_i^2 - 1/2 \int_0^X [W_{i,X}(X)]^2 \, dX \qquad (10)$$

$$W_i(X) = A_{i1} \sinh k_i X + A_{i2} \cosh k_i X + A_{i3} X - \bar{q}_i X^2/(2k_i^2) + A_{i4}. \qquad (11)$$

Regardless of tension or compression in the bar, for each bar there are six constants. These constants are k_i, A_{ij}, $j = 1, 2, \ldots, 5$, $i = 1, 2, \ldots, N$, where N is the number of members. The response of the N-bar frame is known provided that the $6N$ constants can be evaluated. The necessary $6N$ equations are provided from the boundary and joint conditions. The coefficients A_{ij} appear in nonlinear manner only in the expression of $U_i(1)$.

Thus, the boundary and joint conditions containing $U_i(1)$ set up the nonlinear equations in A_{ij}. Therefore, balance of forces in the vertical and horizontal directions, balance of moments, continuity in rotations and continuity in displacements [except those containing $U_i(1)$] lead to a set of linear equations in A_{ij}. Because of this linearity it is possible to eliminate all the constants A_{ij} and end up with N nonlinear equations in the nondimensionalized axial forces k_i.

3.2. *Modeling of connection flexibility*

For the nonlinear connection, the moment–relative rotation behavior is represented by a polynomial model which is taken from Frye and Morris (1975) as,

$$\phi = C_1 M + C_2 M^3 + C_3 M^5 \qquad (12)$$

where ϕ is the relative rotation, M the bending moment and C_i, $i = 1, 2, 3$ are constants (for the case of linear flexible connections $C_2 = C_3 = 0$ and for the case of rigid connections $C_1 = C_2 = C_3 = 0$). For a double web angle connection (connection B) the moment–relative rotation function is given by (Frye and Morris, 1975):

$$\phi = 3.66(kM) \cdot 10^{-4} + 1.15(kM)^3 \cdot 10^{-6}, \qquad (13)$$

where

$$k = d^{-2.4} t^{1.81} g^{0.15},$$

the higher order term (C_3) is neglected, k is a dimensionless factor whose value depends on the size parameters for the particular connected considered and d, t and g are dimensions of connection geometry. For the end plate column stiffener connection (connection A), the moment–relative rotation function is given by:

$$\phi = 1.79(kM)10^{-3} + 1.76(kM)^3 10^{-4}, \qquad (14)$$

where $k = d^{-2.4} t^{-0.6}$.

The corresponding connection geometries are shown in Fig. 2, which also identifies d, t and g for the two types of connections.

3.3. *Buckling equations and related end conditions*

The buckling equations and associated boundary conditions can be obtained by employing a perturbation method (Simitses, 1976) based on the concept of the existence of an adjacent equilibrium position (for either a bifurcation or a limit point). The required steps are as follows: starting with the equilibrium equations and proper boundary conditions expressed in terms of displacements, perturb them by allowing small admissible changes in the displacement functions, make use of equilibrium at a point at which an adjacent equilibrium path is possible, and retain first-order terms in the admissible variations.
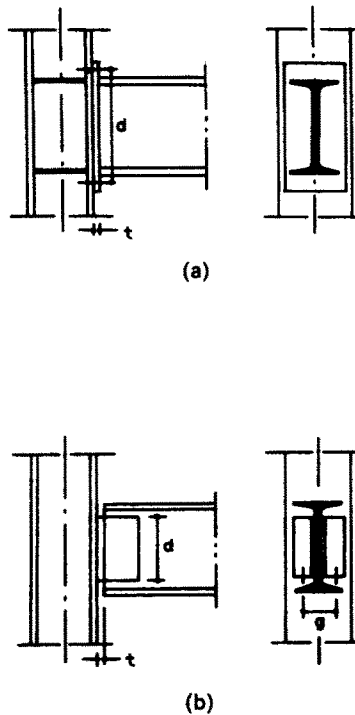
(a)

(b)

Fig. 2. Connection types and standardization parameters. (a) End plate column stiffeners. (b) Double web angle.

Let $\bar{U}_i(X)$ and $\bar{W}_i(X)$ denote the displacement functions on the primary path (equilibrium), and let $U_i^*(X)$ and $W_i^*(X)$ be their infinitesimally small and kinematically admissible variations. Thus, the buckling equations are:

$$U_{i,X}^* + \bar{W}_{i,X} W_{i,X}^* = k_i^*/\lambda_i^2 \tag{15}$$

$$W_{i,XXXX}^* \mp \bar{k}_i^2 W_{i,XX}^* = k_i^* \bar{W}_{i,XX}. \tag{16}$$

The solutions to these equations are:

(for compression)

$$U_i^*(X) = A_{i5}^* + k_i^* X/\lambda_i^2 - \int_0^X \bar{W}_{i,X} W_{,X}^* \, dX \tag{17}$$

$W_i^*(X) = A_{i1}^* \sin \bar{k}_i X + A_{i2}^* \cos \bar{k}_i X + A_{i3}^* X + A_{i4}^*$

$\qquad\qquad + k_i^* X(A_{i2} \sin \bar{k}_i X - A_{i1} \cos \bar{k}_i X + \bar{q}_i X/\bar{k}_i^3)/(2\bar{k}_i),$ (18)

(for tension)

$$U_i^*(X) = A_{i5}^* + k_i^* X/\lambda^2 - \int_0^X \bar{W}_{i,X} W_{,X}^* \, dX \tag{19}$$

$W_i^*(X) = A_{i1}^* \sinh \bar{k}_i X + A_{i2}^* \cosh \bar{k}_i X + A_{i3}^* X + A_{i4}^*$

$\qquad\qquad + k_i^* X(A_{i2} \sinh \bar{k}_i X + A_{i1} \cosh \bar{k}_i X + \bar{q}_i X/\bar{k}_i^3)/(2\bar{k}_i).$ (20)

Note that $\bar{k}_i$ denotes the axial force parameter at the primary equilibrium path at the instant of buckling, and A_{i1} and A_{i2} are the values of the constants to the solution of the equilibrium equations [eqns (6) and (7), on the primary path at buckling].

One may express the additional axial force, $P_i^*(X)$, bending moment, $M_i^*(X)$, and shearing force, $V_i^*(X)$, of member i, in terms of k_i^* and the displacement components $\bar{U}_{ij}(X)$, $\bar{W}_i(X)$, $U_i(X)$ and $W_i^*(X)$. Note that the expressions for W_i^* and U_i^* are linear functions of the constants A_{ij}^*, k_i^*, $j = 1, \ldots, 5$. Also, U_i^*, W_i^* must satisfy the $6N$ end conditions and their satisfaction leads to a system of homogeneous, linear, algebraic equations in the constants k_i^*, A_{ij}^*, ($i = 1, \ldots, N$ and $j = 1, 2, \ldots, 5$). Thus, a nontrivial solution exists if the determinant of the coefficients vanishes. This requirement yields one more nonlinear equation in terms of A_{ij} and k_i and it holds true only at the critical equilibrium point (bifurcation or limit point).

4. INELASTIC EFFECT

The material is assumed to be ideally elastic–plastic and yielding is considered to be concentrated at member ends in the form of plastic hinges (concentrated plasticity). The members are assumed to remain elastic between plastic hinges. Reversals of plastic hinge rotations are not taken into account. The influence of axial force on the moment capacity of the plastic hinge is represented (Kassimali, 1968; Korn and Galambos, 1968) by a bilinear relationship as

$$M_{PC} = M_P \quad \text{for } \frac{|P|}{P_Y} \leqslant 0.15 \tag{21}$$

or

$$M_{PC} = 1.18 M_P \left(1 - \frac{|P|}{P_Y}\right) \quad \text{for } \frac{|P|}{P_Y} > 0.15, \tag{22}$$

in which M_P is the full plastic moment capacity in absence of axial force, M_{PC} is the reduced plastic moment capacity in the presence of axial force and

$$P_Y = F_Y A \tag{23}$$

in which F_Y = yield stress. If the state of the bending moment at any joint of the frame equals or exceeds the plastic moment capacity of the member, a plastic hinge will form. Once a plastic hinge is formed, the member at the hinge can rotate freely and the moment carried by this plastic hinge is assumed to remain unchanged, i.e. plastic hinges are treated as real hinges.

Thus, for example, for a member with a plastic hinge at the middle, the slope continuity (where the plastic hinge is formed) is violated, and the end conditions (equations of continuity in rotation and balance of moments) for the equilibrium equations and buckling equations, will be replaced by

$$M_j(1) = M_{PC}; \; M_j(1) + M_i(0) = 0$$

and

$$M_j^*(1) = 0; \; M_j^*(1) + M_i^*(0) = M_i^*(0) = 0, \quad \text{respectively}$$

(the member is divided into two members, i and j).

5. SOLUTION PROCEDURE

A brief discription of the solution procedure for finding the critical loads and the failure mode is presented below.

From the equilibrium equations, eqns (6) and (7), six constants $(A_{ij}, k_i, j = 1, 2, \ldots, 5,$ $i = 1, 2, \ldots, N$, N is the number of members) are needed to establish the equilibrium response of each member at each load level. For the gabled frame in Fig. 1, 24 unknowns are needed. Close examination of the boundary and joint conditions reveals that these conditions yield $5N$ linear equations in the unknowns A_{ij}, for each member:

$$[C(k_i)]\{A\} = \{D(Q, \varepsilon, k_i)\} \qquad (24)$$

where $[C(k_i)]$ is a $5N \times 5N$ matrix in terms of N k_is, $\{A\}$ is a column matrix of $5N$ coefficients A_{ij} and $\{D(Q, \varepsilon, k_i)\}$ is a column matrix in terms of loads, load eccentricities and k_is. Because of this linearity, it is possible to eliminate all A_{ij} and end up with N nonlinear equations in the N axial force parameters, k_i.

Then, a good initial estimate for the k_is is needed at some low level of the applied load, in order to start the execution of the solution. For a set of assumed values of the N k_i formulate the $[C]$ array and then solve for A_{ij}. The nonlinear equations are checked for satisfaction by the assumed k_i and associated A_{ij} by employing a Quasi-Newton method. One iterates on the value of k_i until the nonlinear equations are satisfied:

$$F_i(k_i, A_{ij}, \ldots) = 0. \qquad (25)$$

The load then is step-increased and the procedure is repeated. The k_i corresponding to the previous load step are employed now as initial estimates for the present load step. Note that at each load level, knowledge of A_{ij} and k_i implies knowledge of the frame response.

As already mentioned in the mathematical formulation section the expressions for the buckling mode, W_i^* and U_i^*, are linear functions of A_{ij}^* and k_i^*. Satisfaction of the corresponding boundary and joint conditions yields a system of $6N$, linear, homogeneous, algebraic equations in A_{ij}^* and k_i^*. For a nontrivial solution to exist, the determinant of the coefficients of A_{ij}^*, k_i^* must vanish. This leads to a critical condition.

At each load level one of the following three cases can be obtained;

(1) Bifurcation point load or limit point load where the determinant changes sign.
(2) Yielding (plastic hinge) where the moment in the member reaches plastic moment capacities (M_{PC}) in the presence of axial load. The plastic hinge is inserted in the structure and the load level is increased.
(3) Bifurcation point or limit point after one or several number of plastic hinges have formed.

The analysis is terminated by buckling instability if the bifurcation point load or limit point load are obtained before the number of plastic hinges is large enough to lead to plastic collapse. The analysis is terminated by plastic collapse if the number of plastic hinges is large enough to develop a plastic mechanism before buckling (limit point or bifurcation).

In the case of realistic flexible connections, the set of nonlinear equations will increase due to nonlinearity in the connections. Thus, in order (for the sake of simplicity) to use the same solution method and equations as for the case of rigid connections, the following concept is introduced.

If the load increments are kept small then the slope to the moment–relative rotation curve at load step $(n+1)$ can be well approximated by the value at load step (n). Then eqn (12) at load level $(n+1)$ is written as

$$\phi_{n+1} = M_{n+1}(C_1 + C_2 M_n^2) \qquad (26)$$

where C_3 is neglected. Clearly then the solution scheme for the case of flexible connections is the same as the one used for rigid connections. For the case of linear elastic rotational
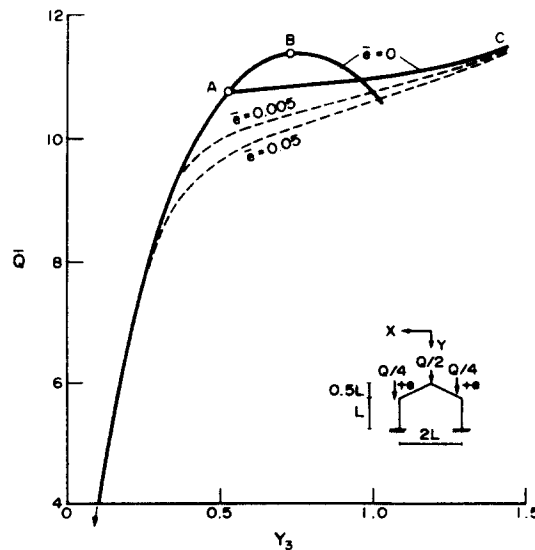
Fig. 3. Fundamental and post-buckling equilibrium paths of a gabled frame for concentrated loads with and without asymmetric eccentricities ($\lambda_1 = 80$, $EI_i = EI_1$).

restraint, the nondimensionalized spring stiffness, $\bar{\beta} = 1/C_1$, is changed from 0 to 10^5 (pin to rigid connection) and the boundary conditions at the supports are given by

$$M_i(0) - W_{i,x}(0)\beta = 0; \quad U_i(0) = 0; \quad W_i(0) = 0. \tag{27}$$

6. NUMERICAL EXAMPLES

6.1. Nonlinear elastic stability analysis

The first example is that of a gabled frame of rise h, of column length L, of distance between the supports S and subjected to concentrated vertical loads near the three joints as shown in Fig. 1.

Figure 3 is typical of the elastic response of gabled frame to transverse loads applied statically near the joints. The results depicted on this figure are for $h/L = 0.5$, $\lambda_1 = 80$, $EI_i/EI_1 = 1$, and clamped boundaries. Curves $OABD$ and OAC correspond to zero load eccentricity, while the dashed curves correspond to $\bar{e} = 0.005$ and 0.05, respectively. These curves are load–deflection curves, where Y_3 is the vertical deflection of joint 3. For this particular geometry sidesway is the mode of buckling at $\bar{Q} = 10.755$. As expected, when there is eccentricity there is no bifurcation, but the response is one that combines bending and axial deformations. This response asymptotically approaches curve OAC.

Figure 4 employs the same geometry and loading but for various ratios of the beam bending stiffness to that of the columns. Clearly, when the beams are stiffer than the columns sway-buckling occurs. On the other hand, for $EI_2/EI_1 < 1(0.5)$, snap-through buckling occurs. Note that these results are for $h/L = 0.5$.

From these two examples it can be concluded that using nonlinear elastic stability analysis, only elastic bifurcation instability or elastic limit point instability can be predicted, which may not represent the true behavior of framed structures.

6.2. Second-order elastic–plastic analysis

An example of a second-order elastic–plastic analysis for the gabled frame is included in Fig. 5. The loading and geometry are shown in the figure. The beams in the frame are analyzed as five elements and the columns are analyzed as one element. A comparison between the present study and experimental results obtained by Majid (1972) is shown in the figure, where Q_{cr}, which appears in the figure, is the predicted experimental value of collapse load. It can be seen that the numerical solutions in the presence of a small imperfection $(0.001Q)$ are in good agreement with the experimental results.

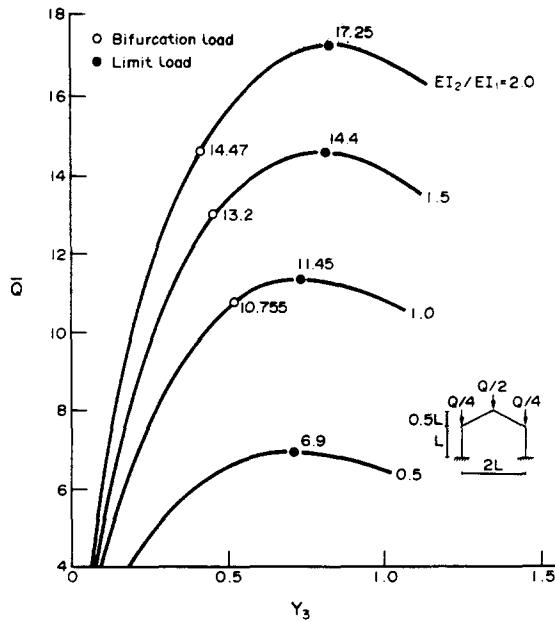From this example it can be seen that only plastic collapse is predicted.

Fig. 4. Effect of stiffness ratio on the critical conditions ($\lambda_1 = 80$).

6.3. Elasto-plastic instability analysis

A first example of elasto-plastic instability analysis is that of a gabled frame, with concentrated loads at the joints, with yield stress $F_Y = 50$ ksi, and slenderness ratio of $\lambda_1 = 100$. All cross-sections for the beams and columns are WF 12×45. The beam and column cross-sections were selected because their sizes were comparable to those used in the actual testing program reported in Frye and Morris (1975). The results of the analysis of the gabled frame with rigid connections and double web angle connections (linear and nonlinear) are shown in Fig. 6. The analysis for the frames with rigid connection and linear connection was terminated by plastic collapse, while for nonlinear connection the analysis was terminated by limit point instability after two plastic hinges.

To study the effect of nonuniform geometry on the behavior of gabled frames, the beams and the columns in the frame are analyzed as three elements and all sections are chosen to be built-up sections with width $b = 8$ in., web thickness $t_w = 0.375$ in. and flange thickness $t_f = 0.625$ in. In order to simplify the problem, constant height along each cross-section is assumed and it varies from 10 in. to 16 in. (the smallest is 10 in., the next one
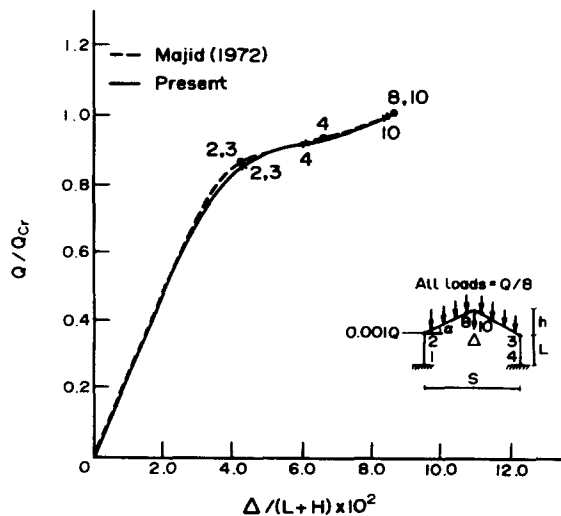

Fig. 5. Load–deflection curves for a gabled frame ($Q_{cr} = 0.555$ kips, $L+h = 22.431$ in., $A = 0.262$ in.^{2}, $EI = 160.488$ kip. in.^{2}, $F_Y = 36$ ksi, $M_P = 1.361$ kip. in., $S = 48$ in., $\alpha = 15°$).
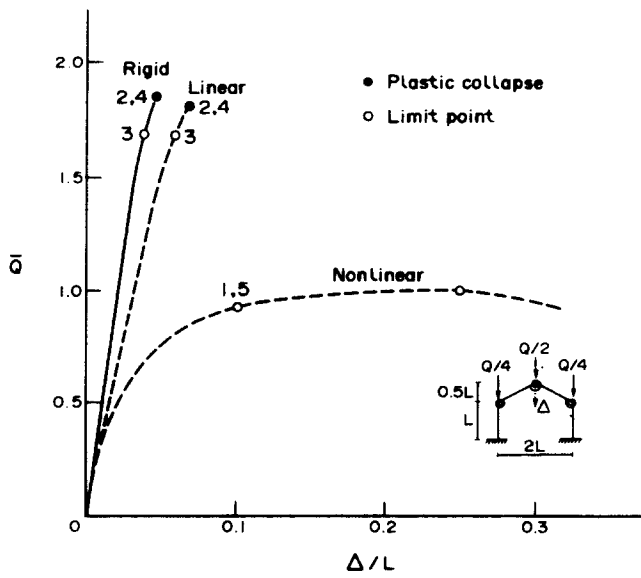
Fig. 6. Effect of the nonlinear flexible connections on the behavior of gabled frame ($\lambda_1 = 100$, $F_Y = 50$ ksi, $E = 29000$ ksi, all section $WF12 \times 45$).
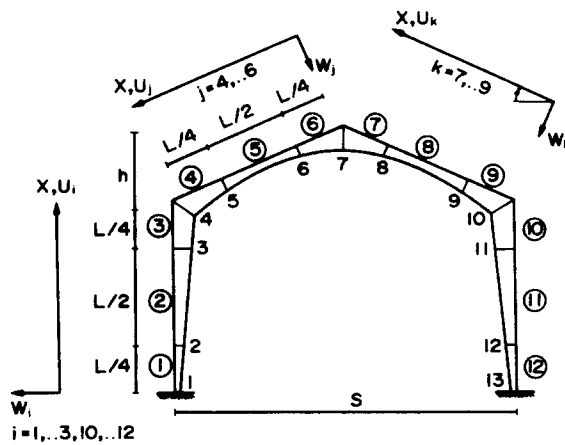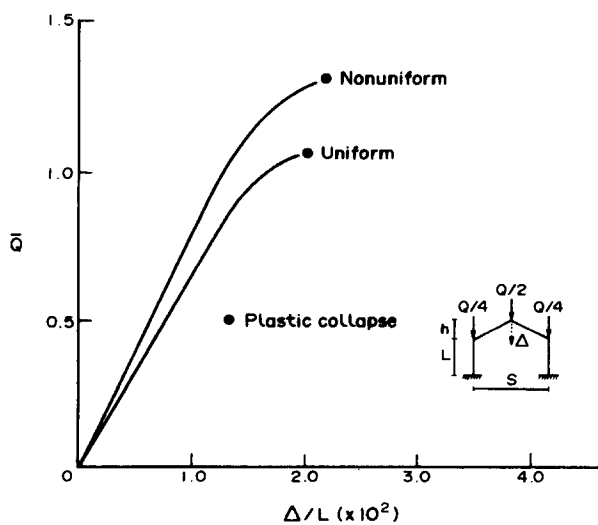

Fig. 7. Geometry and sign convention.

Fig. 8. Effect of nonuniform geometry on the behavior of gabled frame ($E = 29000$ ksi, $F_Y = 50$ ksi, $2h/S = 0.4$, $L = 20$ ft.).
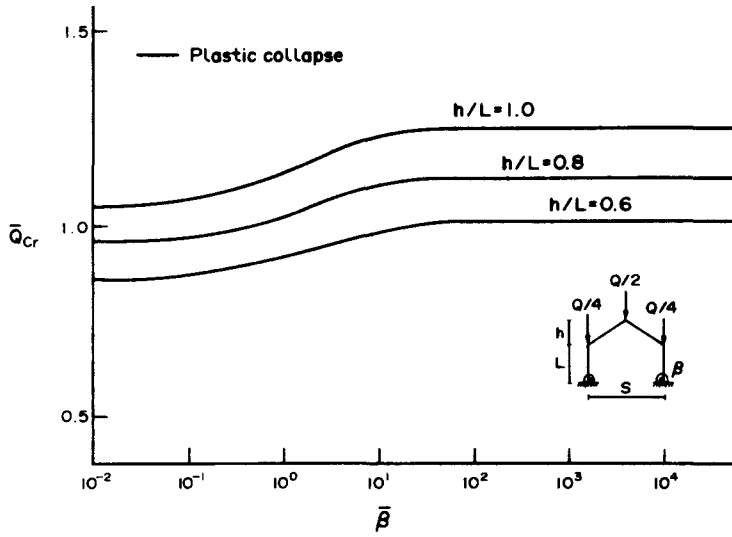
Fig. 9. Load–deflection behavior of a gabled frame with nonuniform geometry using linear and nonlinear connections ($\lambda_1 = 10$, $h/S = 0.4$, $F_Y = 50$ ksi, $E = 29000$ ksi).
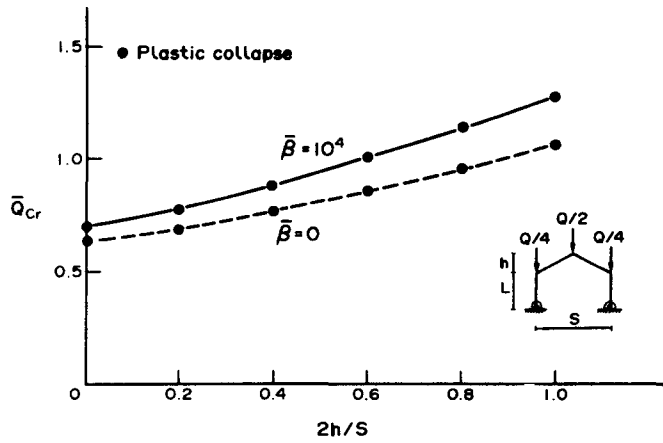

Fig. 10. Effect of rise of gabled frame with nonuniform geometry on the critical load ($E = 29000$ ksi, $\lambda_1 = 10$, $F_Y = 50$ ksi).
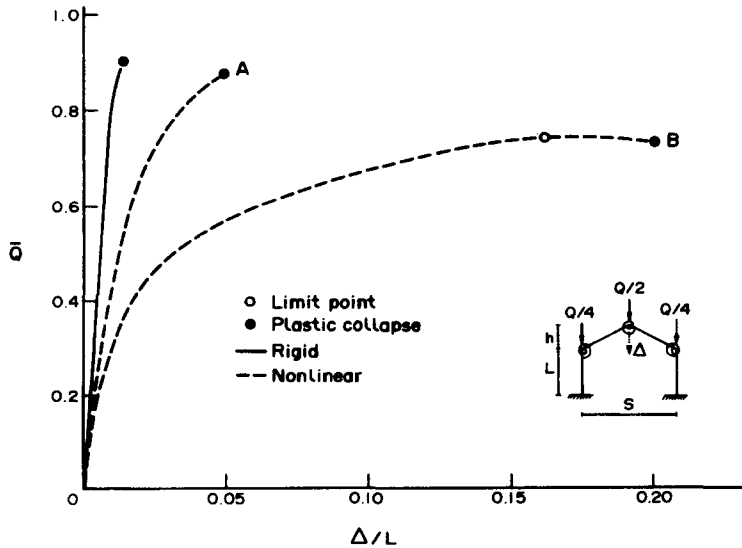

Fig. 11. Effect of the nonlinear flexible connections on the behavior of gabled frame with nonuniform geometry ($\lambda_1 = 10$, $F_Y = 50$ ksi, $E = 29000$ ksi, $2h/S = 0.4$).

12 in. and the largest 16 in.). The shape factor for all the sections is assumed to be 1.18 and the yield stress is equal to 50 ksi (see Fig. 7).

Figure 8 shows a comparison between gabled frames with uniform and nonuniform geometry and with the same weight. The loading and geometry are shown in the figure. It can be seen that by using nonuniform geometry instead of uniform geometry the critical load is increased. For both cases failure modes are due to plastic collapse.

To study the effect of support restraints on the critical loads and failure modes, the analysis is repeated for the gabled frame with rotational restraints (β) at the supports and with $\lambda_1 = 10$. The results are shown, for $2h/S = 0.6$, 0.8 and 1.0, in Fig. 9. For all cases failure is due to plastic collapse.

In order to investigate the effect of rise to span ratio on the critical load and failure mode, the same gabled frame (as in Fig. 9) is analyzed for different values of rise to span ratio ($2h/S = 0$ to 1), $\lambda_1 = 10$ and for both fixed and hinged supports. The results are summarized in Fig. 10. For this case the change of $2h/S$ does not affect the failure mode but it affects the critical load. Failure is by plastic collapse.

To investigate the effect of nonlinear flexible connections on the gabled frame with nonuniform geometry, the example used in Fig. 8 is analyzed for three different types of connections, rigid, end plate connection with column stiffeners (connection A) and double web angle connection (connection B). The results for the three types of connections, loading and geometry are shown in Fig. 11. The analysis for the frame with connection A was terminated by plastic collapse, while for connection B the analysis was terminated by limit point instability after two plastic hinges at the supports. Also, it is observed that the nonlinearity affects both the critical load and the deformation response.

7. CONCLUDING REMARKS

The salient conclusions in the present study may be summarized as follows:

(1) True behavior of gabled frames can be obtained only by incorporating stability and strength.

(2) Use of nonlinear flexible connections affects failure modes, critical loads and deformation response.

(3) Use of linear connections is not acceptable, because it does not approximate well the true connection.

(4) Nonuniform geometry tends to increase the collapse load.

(5) Limit point instability for gabled frames may occur before plastic collapse.

(6) Critical loads and failure modes are affected by support conditions, slenderness ratio, rise to span ratio and type of connection.

REFERENCES

Frye, J. M. and Morris, G. A. (1975). Analysis of flexibly connected steel frames. *Can. J. Civ. Engng* **2**, 280–291.
Huddleston, J. V. (1967). Nonlinear buckling and snap-over of a two-member frame. *Int. J. Solids Structures* **3**(6), 1023–1030.
Jennings, A. and Majid, K. (1965). An elastic–plastic analysis by computer for framed structures loaded up to collapse. *Struct. Engr* **43**(12), 407–412.
Kassimali, A. Large deformation analysis of elastic plastic frames. *J. Struct. Div. ASCE* **109**(ST9), 2107–2314.
Korn, A. and Galambos, T. V. (1968). Behavior of elastic plastic frames. *J. Struct. Div. ASCE* **94**(ST5), 1119–1142.
Kounadis, A. N., Giri, J. and Simitses, G. J. (1977). Nonlinear stability analysis of an eccentrically loaded two-bar frames. *J. Appl. Mech.* **44**(4), 701–706.
Lee, S. L., Manuel, F. S. and Rossow, E. C. (1968). Large deflection and stability of elastic frames. *J. Engng Mech. Div., ASCE* **94**, 521–547.
Lui, E. M. (1985). Effects of connection flexibility and panel zone deformation on the behavior of plane steel frames. Ph.D. Thesis, C. E. Department, Purdue University.
Majid, K. I. (1972). *Nonlinear Structures*, pp. 208–209. Wiley, New York.
Oran, C. (1973). Tangent stiffness in plane frames. *J. Struct. Div. ASCE* **99**(ST6), 973–985.
Qashu, R. K. and Dadeppo, D. A. (1983). Large deflection and stability of rigid frames. *J. Engng Mech. Div., ASCE* **109**(EM3), 765–780.
Simitses, G. J. (1976). *An Introduction to the Elastic Stability of Structures.* Prentice-Hall, Englewood Cliffs, NJ. (Second printing, Krieger, Melbourne, FL, 1985.)

Simitses, G. J. and Giri, J. (1981). Nonlinear analysis of portal frames. *Int. J. Numer. Meth Engng*, **17**, 123–132.

Simitses, G. J. and Kounadis, A. H. (1978). Buckling of imperfect rigid-jointed frames. *J. Engng Mech. Div.*, *ASCE* **104**(EM3), 569–586.

Simitses, G. J. and Mohamed, S. E. (1988). Nonlinear analysis of gabled frames under static loads. *J. Construct. Steel Res.* **11**(4), 338–354.

Simitses, G. J. and Vlahinos, A. S. (1982). Stability analysis of a semi-rigidly connected simple frame. *J. Construct. Steel Res.* **2**(3), 19–32.